JOURNAL OF VIROLOGY, July 2002, p. 6643–6651 Vol. 76, No. 13
0022-538X/02/$04.00+0 DOI: 10.1128/JVI.76.13.6643–6651.2002
Copyright © 2002, American Society for Microbiology. All Rights Reserved.

Antibodies to Rotavirus Outer Capsid Glycoprotein VP7 Neutralize Infectivity by Inhibiting Virion Decapsidation

Juan Ernesto Ludert,[1]* Marie Christine Ruiz,[2] Carlos Hidalgo,[1]† and Ferdinando Liprandi[1]

Centro de Microbiologia[1] and Centro de Biofísica y Bioquímica,[2] Instituto Venezolano de Investigaciones Científicas (IVIC), Caracas 1020-A, Venezuela

Received 23 October 2001/Accepted 2 April 2002

The rotavirus capsid is composed of three concentric protein layers. Proteins VP4 and VP7 comprise the outer layer. VP4 forms spikes, is the viral attachment protein, and is cleaved by trypsin into VP8* and VP5*. VP7 is a glycoprotein and the major constituent of the outer protein layer. Both VP4 and VP7 induce neutralizing and protective antibodies. To gain insight into the virus neutralization mechanisms, the effects of neutralizing monoclonal antibodies (MAbs) directed against VP8*, VP5*, and VP7 on the decapsidation process of purified OSU and RRV virions were studied. Changes in virion size were followed in real time by 90° light scattering. The transition from triple-layered particles to double-layered particles induced by controlled low calcium concentrations was completely inhibited by anti-VP7 MAbs but not by anti-VP8* or anti-VP5* MAbs. The inhibitory effect of the MAb directed against VP7 was concentration dependent and was abolished by papain digestion of virus-bound antibody under conditions that generated Fab fragments but not under conditions that generated $F(ab')_2$ fragments. Electron microscopy showed that RRV virions reacted with an anti-VP7 MAb stayed as triple-layered particles in the presence of excess EDTA. Furthermore, the infectivity of rotavirus neutralized via VP8*, but not that of rotavirus neutralized via VP7, could be recovered by lipofection of neutralized particles into MA-104 cells. These data are consistent with the notion that antibodies directed at VP8* neutralize by inhibiting binding of virus to the cell. They also indicate that antibodies directed at VP7 neutralize by inhibiting virus decapsidation, in a manner that is dependent on the bivalent binding of the antibody.

Rotaviruses, members of the family *Reoviridae*, are an important cause of neonatal diarrhea in humans and in many other animal species. The rotavirus virion is a nonenveloped icosahedral particle, consisting of six proteins organized in three concentric layers containing the genome of 11 segments of double-stranded RNA (30). The outer layer of the virion is composed of 260 trimers of the 37-kDa glycoprotein VP7, the most abundant external protein, which constitute the smooth surface of the virion, and 60 dimeric spikes of the 88-kDa protein VP4 (38, 42). VP7 is a calcium binding glycoprotein; in vitro calcium chelation results in solubilization of the outer layer of the virion (6, 12). The concentration of free Ca^{2+} at which this process occurs is in the range of 10 to 600 nM, depending on the strain (36). Proteolytic cleavage of VP4 into two subunits, VP8* (28 kDa) and VP5* (60 kDa), is necessary for the virus to be infectious (30). Attachment of the virus particles to the cell membrane and penetration have been associated with VP4; however, the role played by VP7 in these events is less clear (7, 15, 26). Recently, it was found that VP4 and VP7 contain sequence binding motifs for members of the α/β integrin family, which have been proposed to mediate rotavirus attachment and entry into cells (16, 17).

Viral neutralization is an in vitro process in which virus binds antibodies and loses infectivity (10, 24). It correlates strongly, although not exclusively, with protection from infection in vivo. Neutralization of rotavirus infectivity has been proposed as an important mechanism of immunological defense against rotavirus infection. Both VP4 and VP7 are targets for the humoral immune response, and they independently elicit neutralizing and protective antibodies (20). Passive protection against rotavirus-induced diarrhea has been achieved in experimental mouse models by using monoclonal antibodies (MAbs) against VP4 and VP7 (29). More recently, MAbs of the immunoglobulin A (IgA) subtype directed against VP8* were found to neutralize apically administered virus after transcytosis from the basolateral to the apical domain of polarized epithelial cells and to protect newborn mice from diarrhea in a "backpack tumor" model (33). The antigenic structure of the rotavirus virion is complex, and at least two mechanisms of antibody-mediated neutralization have been proposed. Ruggeri and Greenberg (32) identified distinct patterns of neutralization when comparing the neutralizing activity of a panel of MAbs directed against VP4 and VP7, and they concluded that antibodies directed against VP8*, but not against VP5* or VP7, neutralized virus infectivity by inhibiting viral binding. More recently, Zhou et al. (43) identified a series of MAbs capable of inducing conformational changes upon binding to VP8*, which in turn induced particle disassembly. They proposed virion disruption as a novel mechanism for rotavirus neutralization. However, the most efficient rotavirus-neutralizing antibodies described to date are all directed against VP7, and very little is known of the neutralization mechanism via this glycoprotein. Dormitzer et al. (12) hypothesized that neu-

* Corresponding author. Mailing address: Center for Microbiology and Cell Biology, IVIC Apdo. 21827, Caracas 1020-A, Venezuela. Phone: 58-212-5041489. Fax: 58-212-5041382. E-mail: jeludert@ivic.ve.

† Present address: Department of Structural Biology, IVIC Apdo. 21827, Caracas 1020-A, Venezuela.

TABLE 1. Designations, isotypes, specificities, and neutralizing capacities of MAbs

MAb	Isotype	Reactivity[a] to:		Protein	Position[b]	Region or loop[c]	Neutralizing capacity
		RRV	OSU				
159	IgG1	+++	−	VP7	94	A	Yes
M60	IgG1	+++	+++	VP7	ND	ND[d]	No
1A9	IgG1	++	−	VP8*	100	3	Yes
7A12	IgG1	++	−	VP8*	188	9	Yes
2G4	IgG1	+++	+	VP5*	393	Fusion domain	Yes
1C10	IgG1	−	+++	VP7	96	A	Yes
4B5	IgG	−	++	VP8*	100	3	Yes
5G7	IgG	−	++	VP8*	125	5	Yes
4E8	IgG	−	+	VP8*	125	5	Yes
4B2	IgG2a	++	++	VP6	ND	ND	No

[a] Reactivities of neutralizing MAbs were determined by neutralization assays; reactivities of nonneutralizing MAbs were determined by immunohistochemistry on rotavirus-infected cells. +++, titer of >1:10,000; ++, titer of >1:2,000; +, titer of >1:200; −, titer of <1:100. ND, not determined.
[b] Based on mutations conferring resistance to neutralization.
[c] Regions on VP7 are as described by Ciarlet et al. (5); loops on VP8* are based on secondary structure predictions by Isa et al. (21).
[d] MAb M60 binds to an epitope distinct from all neutralization domains (39).

tralizing MAbs binding to VP7 on the virion may prevent calcium chelation and solubilization of VP7.

Elucidation of the mechanisms of rotavirus neutralization is important not only for immunization purposes but also because such information may help in the understanding of the early events of rotavirus infection. This paper reports results which are consistent with the notion that antibodies directed at VP8* neutralize by inhibiting the binding of rotavirus to the cell and which indicate that antibodies directed at VP7 neutralize rotavirus infectivity by inhibiting virion decapsidation.

MATERIALS AND METHODS

Cells and viruses. Rotavirus strains OSU and RRV were multiplied in MA-104 cells in the presence of trypsin as previously described (5). MA-104 cells were grown in minimal essential medium (MEM) supplemented with 10% fetal calf serum. All the experiments were performed with virions purified by cesium chloride gradient isopycnic centrifugation. For virus production, infected cells were freeze-thawed twice after nearly complete cytopathic effect and the resulting virus suspension was clarified by low-speed centrifugation for 20 min at 4,000 × *g*. The supernatant was treated with 7% polyethylene glycol 8000 and 2.2% NaCl for 18 h at 4°C under agitation. The virus was pelleted by centrifugation for 30 min at 8,000 × *g*. Pellets were suspended in 0.1 M phosphate-buffered saline (PBS) supplemented with 2 mM $CaCl_2$ (PBS-Ca), and the virus was concentrated by pelleting through a 45% sucrose cushion in PBS-Ca for 3 h at 83,000 × *g*. The pellets were suspended in PBS-Ca, mixed with a CsCl solution in PBS-Ca (1.377 g/ml), and centrifuged at 151,000 × *g* for approximately 48 h at 7°C. Bands corresponding to triple-layered virus particles (TLP) and double-layered virus particles (DLP) were collected from the top of the gradient with Pasteur pipettes. Virus particles were desalted by several washes with PBS-Ca by using microcentrifuge filters with a 300,000-molecular-weight cutoff (Millipore) according to the manufacturer's instructions. Virus concentrations were quantitated by measuring absorbance at 280 nm, and virus titers were determined by an immunoperoxidase focus-forming assay as described below. The OSU and RRV purified preparations used contained titers of 6×10^9 focus-forming units (FFU)/ml with a concentration of 200 μg/ml and 1×10^8 FFU/ml with a concentration of 40 μg/ml, respectively.

MAbs. MAbs against OSU VP4, fragment VP8* (4B5, 5G7, 4E8), VP7 (1C10), and VP6 (4B2) have been described previously (5, 25). MAbs against RRV VP4, fragment VP8* (7A12, 1A9) and fragment VP5* (2G4), and VP7 (159, M60) were the kind gift of Harry Greenberg (Stanford University, Palo Alto, Calif.) and have been described previously (39). MAbs 159 and M60 were used as ascites fluids; the other MAbs were purified from ascites fluids with a protein G-Sepharose column (Pharmacia, Inc.). Immunoglobulin concentrations of purified MAbs were determined by measuring absorbance at 280 nm. Antibodies were stored at −20°C. Table 1 summarizes the characteristics of the MAbs used in this study.

Neutralization assays. Neutralization assays were performed basically as described by Ruggeri and Greenberg (32). In brief, purified OSU virions were diluted in MEM to a concentration of 20 ng/ml (2×10^5 FFU/ml). A range of antibody concentrations from 0.06 to 60 μg/ml was prepared by making threefold dilutions of each MAb in MEM. Equal volumes (100 μl) of the viral suspension and the MAb dilutions were incubated for 90 min at 37°C. The residual infectivity after neutralization was determined in duplicate in monolayers of MA-104 cells grown in 96-well plates and infected with 100 μl of serially diluted (10-fold) reaction mixtures. After 90 min of virus adsorption at 37°C, the inoculum was removed, and 100 μl of fresh MEM was added to the cells. Cells were incubated at 37° under a CO_2 atmosphere until the next day (12 to 18 h postinfection [p.i.]) and then were fixed with cold methanol and immunostained for FFU by using a peroxidase-conjugated MAb directed against VP6 as a primary antibody. Rotavirus-infected cells were counted, and infectivity in the presence of antibodies was expressed as a percentage of the infectivity obtained in the absence of antibodies (2, 26).

Light-scattering assays. The TLP-to-DLP transition of virions bound or not to the different MAbs in controlled calcium concentrations was monitored by 90° light scattering. For a given concentration of virus particles, the magnitude of the dispersed light is related to the radius of the particles. Aliquots (10 μl) of purified OSU (200 μg/ml) or RRV (40 μg/ml) virions were mixed with 2 μl of different MAbs (see figure legends for MAb concentrations), and the mixtures were incubated for 1 h at room temperature. The mixtures were introduced into the stirred cuvette of a spectrofluorimeter (model MP1; Photon Technology International Inc.) that contained 1.1 ml of a buffered Ca^{2+} solution. Solutions of a defined free Ca^{2+} concentration were obtained by mixing different proportions of two media containing 100 mM KCl–10 mM morpholinepropanesulfonic acid (MOPS) at pH 7.2 supplemented with 10 mM EGTA or 10 mM Ca-EGTA, respectively (Molecular Probes). The free Ca^{2+} concentration was calculated from the equilibrium equation for Ca-EGTA at 25°C by using a K_d of 150 nM. Slits were adjusted to 0.5 to 1 nm. Scattering was measured by setting both monochromators of the fluorimeter at a wavelength of 300 nm. Results are presented as relative scattering (expressed as a percentage), calculated as $(S_t - S_0)/(S_m - S_0) \times 100$, where S_0 is the minimal scattering determined at the end of each experiment by addition of an excess of EGTA, S_t is the signal at a time *t*, and S_m is the maximal scattering attained after addition of the rotavirus suspension.

The infectivity of each virus-antibody mixture was assayed in parallel experiments by making 10-fold serial dilutions of the mixtures in MEM and inoculating 100 μl of each dilution in triplicate onto MA-104 cells grown in 96-well plates to measure FFU. Results are expressed as percentages of the control infectivity, as described for the neutralization assays (2, 26).

Papain digestion. For digestion of the anti-VP7 MAb bound to virions, virus-antibody mixtures were treated with papain as described by Johnstone and Thorpe (22), with modifications. In brief, after incubation for 1 h of the OSU-MAb 1C10 mixtures prepared as described above, duplicates were treated with 3 μl of preactivated papain (3.3 μg/μl) for 3 h at room temperature. Since the anti-VP7 MAb used is of the IgG1 subclass (3), digestion with papain was carried out either in the presence of a reducing agent (10 mM cysteine, 0.1 M sodium phosphate [pH 6.5], 20 μM $CaCl_2$), to obtain Fab fragments, or in the absence of a reducing agent (0.1 M sodium phosphate [pH 6.5], 20 μM $CaCl_2$), to obtain $F(ab')_2$ fragments. The reaction was stopped by addition of iodoacetamine (Sigma) to 1.5 mM, and the mixtures were kept in ice until they were added to the

cuvettes. Papain (Sigma) was preactivated by incubation of 5 mg in 1 ml of 10 mM cysteine–0.1 M sodium phosphate (pH 6.5)–2 mM EDTA at 37°C for 30 min, followed by removal of the reducing agent and EDTA by desalting on a Sephadex G-25 minicolumn (Pharmacia).

EM analysis of OSU-MAb complexes. Purified OSU virions were diluted in MEM to give a concentration of 3 μg/ml. A range of antibody concentrations from 2,640 to 2.64 μg/ml was prepared by making 10-fold dilutions of MAb 1C10 in MEM. Equal volumes (10 μl) of the viral suspension and the MAb dilutions were incubated for 1 h at room temperature. Aliquots (10 μl) of each mixture were observed directly at the electron microscope (EM). Ionized and collodion-carbon-coated grids were floated over the aliquots at room temperature for 5 min, and the grids were stained with 2% phosphotungstic acid (PTA; pH 6.5) and examined at the EM (27). The rest of the mixture (10 μl) was serially diluted with MEM (10-fold), inoculated onto MA104 cell monolayers in 96-well plates, and assayed for residual infectivity as described above for neutralization assays.

EM analysis of RRV-MAb complexes treated with EDTA. Aliquots of the RRV preparation and the RRV-MAb 159 mixture used for the light-scattering assays were analyzed by EM. Samples were suspended in PBS–1.8 mM Ca^{2+} or in PBS–10 mM EDTA for 10 min and were observed under the EM after negative staining (25).

Transfection of antibody-rotavirus complexes into MA-104 cells. Transfection experiments were performed as described by Bass et al. (2), with modifications. Purified OSU virions (10^7 FFU/ml) were mixed with 2 μl of a purified anti-VP4 (5G7), anti-VP7 (1C10), or anti-VP6 (4B2) MAb for 1 h at 37°C. After incubation, each mixture was divided into two 50-μl aliquots. One aliquot was mixed with 50 μl of 100-μg/ml Lipofectin (Gibco), vortexed briefly, and incubated at room temperature for 20 min; the other aliquot was treated with 50 μl of MEM as a control. Each mixture was subsequently diluted up to 200 μl with MEM and then serially diluted (10-fold) in MEM; 100 μl of each dilution was inoculated in duplicate onto MA-104 cells grown in 96-well plates to measure FFU. Results are expressed as percentages of the infectivity present in the nontransfected virus preparation that was not reacted with antibodies.

RESULTS

Neutralization of OSU by anti-VP7 and anti-VP4 MAbs. Previous work (32) has indicated that on a mass basis, MAbs directed against VP7 of strain RRV show substantially more neutralizing activity than MAbs directed against VP4. Moreover, the anti-VP7 and anti-VP4 MAbs showed differences in their neutralization kinetics. We tested whether these results could be confirmed with a different virus-MAb combination by using the OSU strain of porcine rotavirus (Fig. 1). For MAb 1C10 directed against VP7, an abrupt and maximal neutralizing activity, more than 3 $\log_{10}$ units, was attained at a MAb concentration of 0.3 μg/ml. On the other hand, at this concentration, MAb 5G7, directed against VP4 (VP8*), reduced infectivity by only 1 $\log_{10}$ unit. Further increases in the concentration of MAb 5G7 showed a gradual decrease in the number of FFU, and the maximum reduction of infectivity was approximately 3 $\log_{10}$ units, at a concentration of 30 μg/ml. MAb 4E8, a weak neutralizing antibody directed against VP4 (VP8*), showed no effect at concentrations up to 1 μg/ml. At higher concentrations, MAb 4E8 induced a small effect, reaching a reduction of 1 $\log_{10}$ unit in the number of FFU at the maximum antibody concentration used (30 μg/ml).

Analysis of the decapsidation process by light scattering. Perpendicular light scattering allows the observation in real time of the changes in particle size that accompany the TLP-to-DLP transition (36). Figure 2 shows the time course of light scattering upon addition of purified OSU or RRV virions to media containing different free Ca^{2+} concentrations. At a free Ca^{2+} concentration of 40 μM, there was no change in the scattering signal when OSU virions were added. At 150 nM Ca^{2+}, the scattering signal decreased, indicating the solubilization of the outer layer of the capsid. This process was much faster at a free Ca^{2+} concentration of zero, obtained with 10 mM EGTA (Fig. 2, left panel). For the RRV strain, this transition was not observed at concentrations above 150 nM but was easily detectable at 26 nM Ca^{2+}. The transition became faster as the concentration of Ca^{2+} decreased to zero (10 mM EGTA) (Fig. 2, right panel). This indicates that the outer capsid of OSU virions requires a higher concentration of free Ca^{2+} for stability than the outer capsid of the RRV virion. The difference in calcium-dependent stability between the outer capsid layers of different strains is in agreement with previous reports (14, 36).

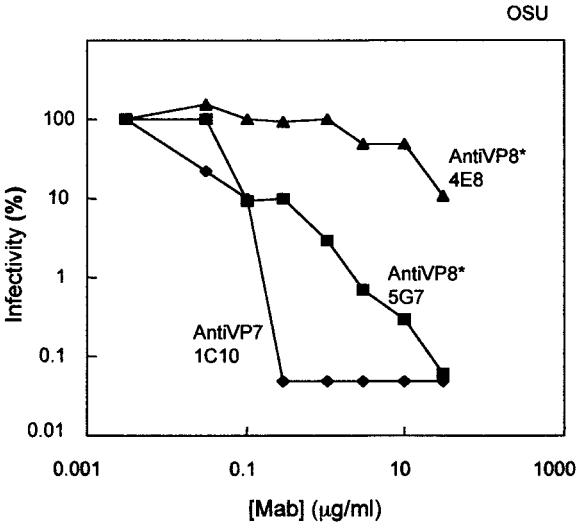

FIG. 1. Neutralization of OSU infectivity by MAbs directed at VP7 (1C10) and VP8* (4E8 and 5G7). Purified OSU virions (100 μl; 20 ng/ml; 2×10^5 FFU/ml) were mixed with purified MAbs (100 μl) at different concentrations (0.06 to 60 μg/ml) and incubated at 37°C for 1.5 h. Virus-antibody mixtures were serially diluted and inoculated in duplicate onto MA-104 cells grown in 96-well plates. After further incubation at 37°C for 1.5 h, the inoculum was removed and fresh MEM was added to the cells. The next day (12 to 18 h p.i.), the cells were fixed with methanol and immunostained for FFU. Results are expressed as percent residual infectivity after neutralization compared with the infectivity of the virus incubated without antibodies. Results from one experiment are shown. The experiment was repeated twice with similar results.

Kinetics of decapsidation of neutralized OSU and RRV virions. We showed above that the neutralization efficiencies of MAbs directed against VP7 and VP4 of OSU are very similar to those previously reported for strain RRV (32). Therefore, we studied the effects of neutralizing MAbs on the in vitro decapsidation process for these two rotavirus strains. Neutralizing MAbs 1C10 and 159 against VP7, specific for strains OSU and RRV, respectively, were tested. These MAbs completely inhibited the decapsidation of purified OSU and RRV virions in vitro observed at Ca^{2+} concentrations of 150 and 26 nM, respectively (Fig. 3). Addition of 10 mM EGTA to reduce free Ca^{2+} from 150 to 50 nM rapidly induced decapsidation of the 1C10-neutralized OSU virus (Fig. 3, top panel). For RRV, reduction of the free Ca^{2+} concentration from 26 to 10 nM by addition of EGTA (10 mM) did not reverse the effect of MAb 159. This suggests that the Ca^{2+} concentration necessary for decapsidation of the RRV-MAb 159 complex is below 10 nM. These results show that neutralizing MAbs directed against

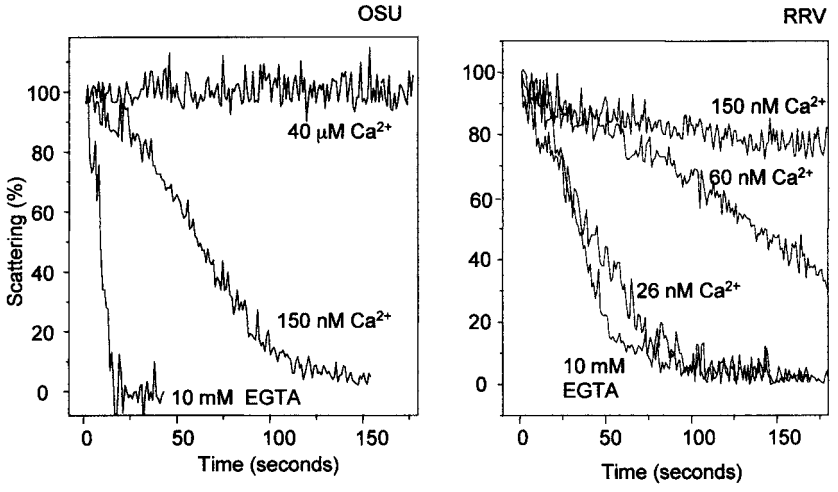

FIG. 2. Kinetics of decapsidation of purified OSU (left) and RRV (right) virions at different Ca^{2+} concentrations, as analyzed by perpendicular light scattering. Ten microliters of purified OSU (200 μg/ml) or RRV (40 μg/ml) virions was added to a stirred cuvette containing 1.1 ml of EGTA–Ca-EGTA buffers adjusted to various Ca^{2+} concentrations (as indicated) and maintained at 25°C (see Materials and Methods). Results are presented as relative scattering as described in Materials and Methods. Results of one experiment from a series of two are shown.

VP7 induce a change in the Ca^{2+} concentration needed to effect the TLP-to-DLP transition, and they suggest an increase in the affinity of the outer layer for Ca^{2+}. This change in affinity is not due to the mere binding of the antibodies to VP7, since no inhibition of decapsidation by the nonneutralizing MAb M60, directed against RRV VP7, was observed (Fig. 3, bottom panel). None of the neutralizing MAbs directed against VP4 showed any effect on the rate of virion decapsidation at the concentrations tested. OSU virions that were reacted with the neutralizing MAb 5G7, which recognizes VP8*, showed a kinetics of decapsidation similar to that of the control, unreacted virions (Fig. 3, top panel). MAbs 4B5 and 4E8, directed against OSU VP8*, and MAb 2G4, directed against OSU VP5*, had no effect when tested at concentrations of 534, 272, and 200 μg/ml, respectively (data not shown). Similarly, neutralizing MAbs 7A12 and 2G4, which recognize VP8* and VP5* of RRV, respectively, also showed a kinetics of decapsidation indistinguishable from that of the control (Fig. 3, bottom panel). MAb 1A9 (200 μg/ml), directed against RRV VP8*, also showed a lack of inhibition (data not shown).

The virus-antibody mixtures were titrated in parallel on MA-104 cells. Neutralizing MAbs directed at VP7 of either OSU or RRV reduced the infectivity of the mixture by 5 to 6 log units, while neutralizing MAbs directed against VP4 reduced the infectivity of the mixture by 1 to 3 log units (data not shown).

Since neutralization of viral infectivity by MAbs directed against VP7 is concentration dependent (see Fig. 1), we studied the effect of antibody concentration on the kinetics of decapsidation of purified OSU virions (Fig. 4). Ten microliters of purified virions (200 μg/ml) was mixed with 10-fold dilutions of MAb 1C10. At a MAb concentration of 528 μg/ml in the reaction mixture, decapsidation of the virus was totally prevented in a 150 nM Ca^{2+} medium. At a 10-fold-lower concentration of MAb 1C10 (52.8 μg/ml), the TLP-to-DLP transition occurred with a lag and at a very low rate. At a final MAb concentration of 5.3 μg/ml, the antibody was no longer capable of preventing decapsidation, and the rate was indistinguishable from that observed for the control without antibody.

Effect of papain digestion of a virus-bound MAb on the kinetics of decapsidation. Ruggeri and Greenberg (32) demonstrated that the neutralization capacity of MAbs directed against VP7 was dependent on the bivalent binding of the antibody. Therefore, we studied the effect of papain digestion on the capacity of MAb 1C10 to prevent the decapsidation of OSU in vitro. We took advantage of the fact that this MAb is of the IgG1subclass (4) and carried out the digestion with preactivated papain in the presence or absence of a reducing agent to obtain monovalent Fab fragments or bivalent $F(ab')_2$ fragments, respectively (22). Figure 5 shows that MAb 1C10 loses its capacity to prevent decapsidation when digestion is carried out in the presence of the reducing agent cysteine to generate Fab fragments, while $F(ab')_2$ fragments still retain their capacity to prevent decapsidation. Infectivity assays carried out in parallel for each preparation showed that the neutralizing capacity of the Fab fragments was 300- to 1,000-fold lower, and that of the $F(ab')_2$ fragments was 20- to 50-fold lower, than that of the intact MAb (data not shown).

Kinetics of neutralization and aggregation of OSU virus. Since neutralization and inhibition of the TLP-to-DLP transition induced by antibodies to VP7 are dependent on bivalent binding, we evaluated a possible role for virion aggregation in these processes. Purified OSU (1.5 μg/ml) and MAb 1C10 at different concentrations were incubated, and aliquots of the mixture were analyzed by EM and infectivity assays (Fig. 6). At MAb concentrations of 1,320 and 132 μg/ml, infectivity was reduced by 4 to 5 log units and no virion aggregation was observed. Virion aggregation (up to 90% of the virus particles) and a 0.5-log-unit reduction in infectivity were observed at a MAb concentration of 13.2 μg/ml. At a lower MAb concentration (1.32 μg/ml), neither neutralization nor aggregation was observed. These results indicate a dissociation between virion agglutination and neutralization with anti-VP7 MAbs (Fig. 6A and B). On the other hand, a tight correlation between neutralization and inhibition of decapsidation was observed when the percentages of infectivity (Fig. 6B) and decapsidation (Fig. 4) were plotted as functions of the MAb/virus

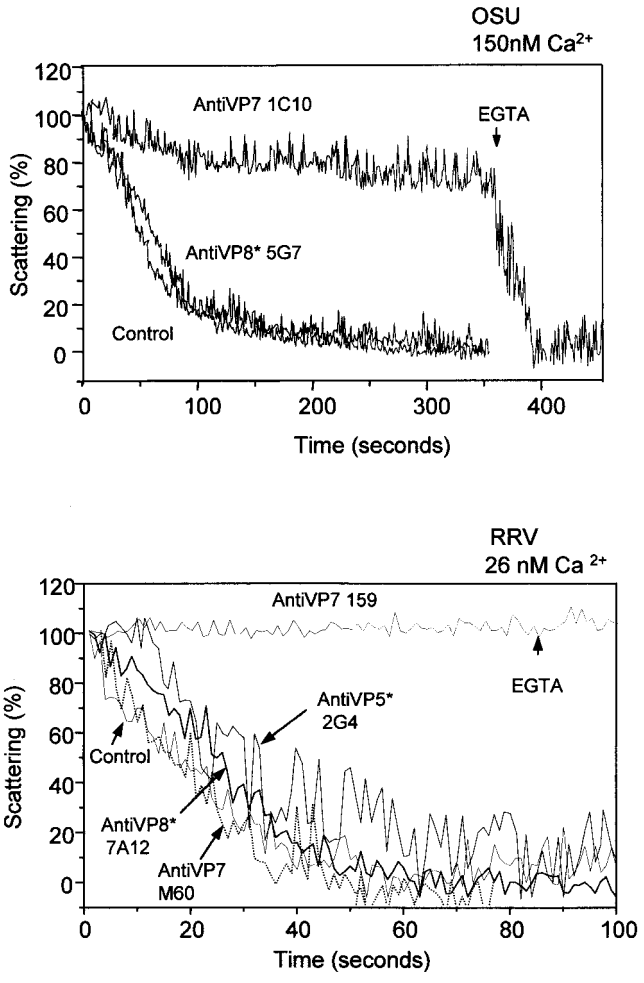

FIG. 3. Kinetics of decapsidation of purified OSU (top panel) and RRV (bottom panel) virions neutralized by MAbs directed at VP7 and VP4. Purified OSU (10 μl; 200 μg/ml) or RRV (10 μl; 33 μg/ml) virions were mixed with different MAbs (2 μl) and incubated for 1 h at room temperature. The concentration of each MAb in the mixture (in micrograms per milliliter) was as follows: for 1C10, 528; for 5G7, 580; for 159, approximately 500; for M60, approximately 500; for 2G4, 222; and for 7A12, 440. Virus-antibody mixtures (12 μl) were added to a stirred cuvette containing 1.1 ml of EGTA–Ca-EGTA buffers adjusted to the Ca^{2+} concentrations indicated above the panels and were maintained at 25°C. EGTA (10 mM) was added as indicated (arrows) to the OSU virus to reduce the Ca^{2+} concentration from 150 to 50 nM and to the RRV virus to reduce the Ca^{2+} concentration from 26 to 10 nM. MAbs used are indicated. Results of one experiment from a series of three are shown.

ratio (Fig. 6C), suggesting a close association between these two events.

EM analysis of rotavirus-MAb complexes. The results obtained in the light-scattering assays with strain RRV were confirmed by EM analysis. The results showed that RRV TLP were disassembled and converted to DLP after treatment with 10 mM EDTA to reduce the free Ca^{2+} concentration to zero (Fig. 7A, B, and C). In contrast, RRV TLP that were reacted with MAb 159 (Fig. 7D) were stable, since they were resistant to decapsidation by the medium devoid of Ca^{2+} (PBS-EDTA) (Fig. 7E).

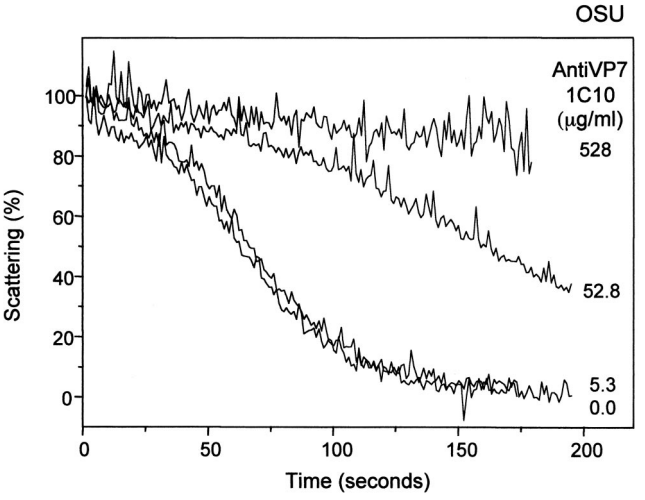

FIG. 4. Kinetics of decapsidation of purified OSU virions reacted with different concentrations of purified MAb 1C10 directed against VP7. Purified OSU (10 μl; 200 μg/ml) virions were mixed with different concentrations of MAb 1C10 (2 μl) and incubated for 1 h at room temperature. Virus-antibody mixtures (12 μl) were added to a stirred cuvette containing 1.1 ml of EGTA–Ca-EGTA buffers adjusted to a 150 nM Ca^{2+} concentration and maintained at 25°C. MAb concentrations in the mixture are indicated. Results of one experiment from a series of two are shown.

Lipofection of neutralized OSU. Previous studies suggest that the transit of the virion through a low-calcium environment during entry is a requirement for virion decapsidation (27, 37). Since the calcium concentration of the cytoplasm is presumably low enough to destabilize the OSU rotavirus outer capsid, we used Lipofectin to directly deliver neutralized virus

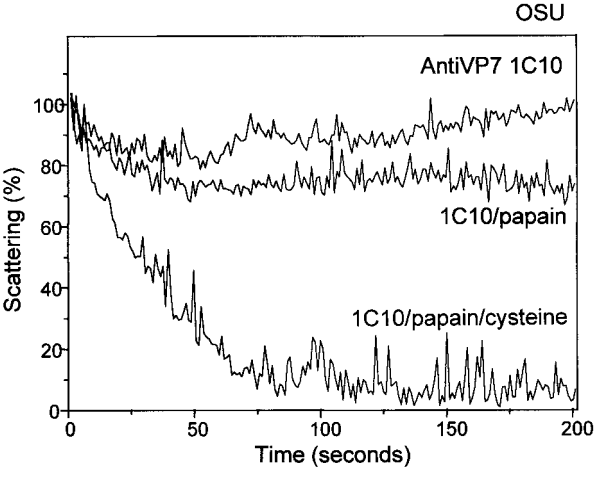

FIG. 5. Effect of papain digestion on decapsidation of purified OSU virions neutralized by MAb 1C10, directed against VP7. Purified OSU (10 μl; 200 μg/ml) virions were mixed with purified MAb 1C10 (2 μl; 2,640 μg/ml) and incubated for 1 h at room temperature. Virus-antibody mixtures were treated with papain (0.8 mg/ml) for 3 h at room temperature in the presence or absence of a reducing agent (10 mM cysteine). After the reaction was stopped with iodoacetamide (1.5 mM), the mixtures were added to a stirred cuvette containing 1.1 ml of EGTA–Ca-EGTA buffers adjusted to 150 nM Ca^{2+} and were maintained at 25°C. The MAb and digestion conditions used are indicated. Results of one experiment from a series of two are shown.

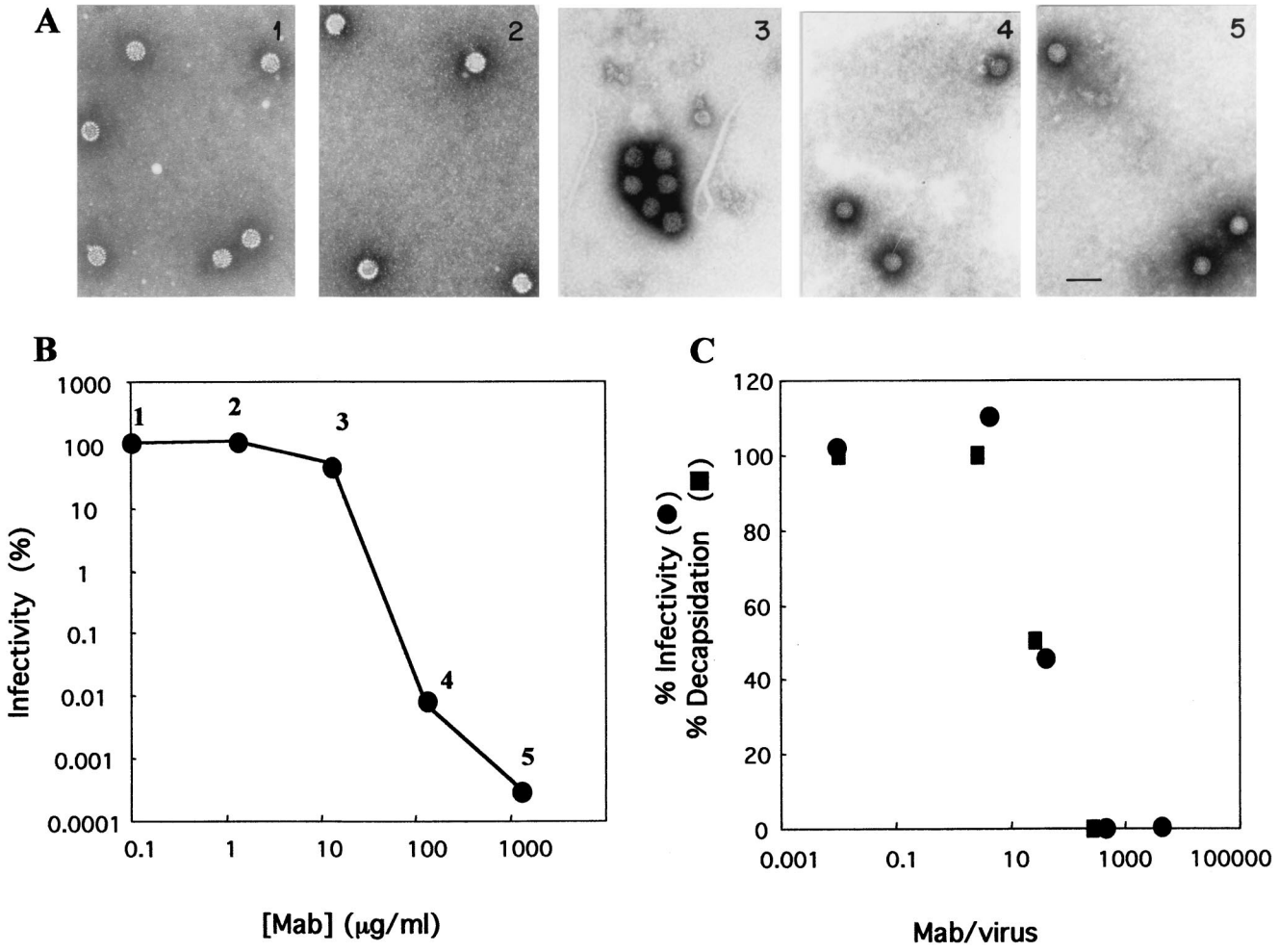

FIG. 6. Kinetics of neutralization and aggregation of OSU virus. Purified OSU (3 μg/ml) virions were mixed with MAb 1C10 at different concentrations and incubated for 1 h at room temperature. (A) Aliquots of each virus-antibody mixture were observed directly by EM. Each mixture was identified by a number from 1 to 5. Bar, 100 nm. (B) The same virus-antibody mixtures for which images are shown in panel A were diluted, inoculated onto MA-104 cell monolayers in 96-well plates, and assayed for residual infectivity. Results are expressed as percent residual infectivity after neutralization compared with the infectivity of the virus incubated without antibodies. (C) Residual infectivity after neutralization (data from Fig. 6B) and inhibition of decapsidation after incubation with different MAb 1C10 concentrations (data from Fig. 4) were plotted as functions of the MAb/virus ratio.

into the low-calcium environment of the cytoplasm. Previous control experiments indicate that lipofection efficiently delivers DLP and TLP into the cell cytoplasm to induce rotavirus replication (2). We reasoned that viruses neutralized via VP7 would remain noninfectious even after delivery into the cytoplasm, while viruses neutralized via VP4 would regain infectivity once the cell plasma membrane was bypassed. Figure 8 shows that the infectivity of a rotavirus neutralized with a MAb directed against VP7 (1C10) could not be recovered after lipofection. The infectivity of the neutralized rotavirus with or without Lipofectin was less than 0.1% of the infectivity of the control nonneutralized preparation (Fig. 8, MEM). In contrast, the infectivity of the virus preparation neutralized with MAb 5G7, directed against VP8*, could be partially recovered upon lipofection, increasing sevenfold in relation to the infectivity of the untreated virus. A control preparation that reacted with a MAb directed against VP6 (4B2) showed a slight increase in infectivity upon treatment with Lipofectin. The infectivity observed in the transfected preparation of OSU virions neutralized via VP8* could not be attributable to contaminating DLP, since infectivity was not recovered when the anti-VP7 MAb 1C10 was used.

DISCUSSION

Neutralization is considered one of the key mechanisms involved in the inhibition of viral infectivity mediated by antibodies. There are several mechanisms by which antibodies inactivate viruses (10, 24). These include inhibition of attachment of the virus to the receptor on the target cell and inhibition of events that occur post-cell attachment. Each virus-cell system presents its own unique properties; furthermore, several mechanisms may be operating for the neutralization of any one virus (10). MAbs directed against both outer capsid rotavirus proteins, VP4 and VP7, show potent neutralizing activity; however, the mechanisms of neutralization mediated by these

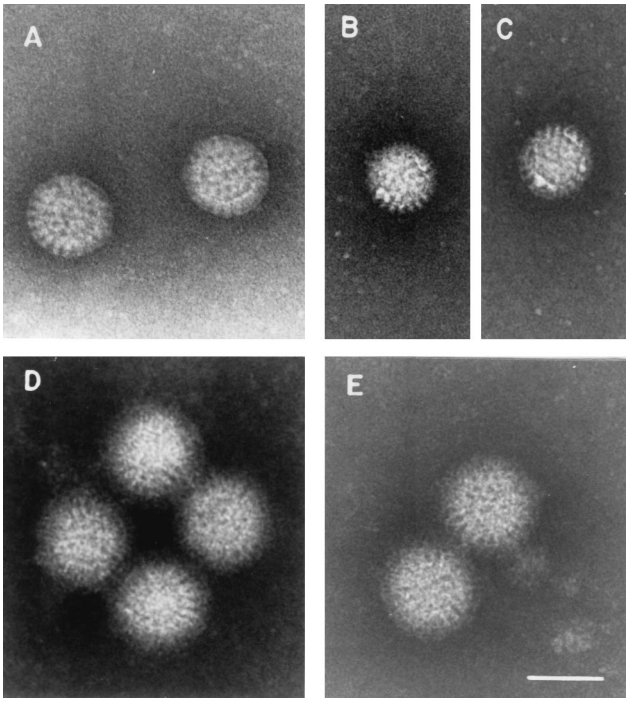

FIG. 7. EM analysis of RRV-anti-VP7 MAb complexes. Purified RRV virions were incubated with PBS–2 mM Ca^{2+} (A) or PBS–10 mM EDTA (B and C) for 10 min at room temperature. Purified RRV virions (33 μg/ml) reacted with the anti-VP7 MAb 159 (500 μg/ml) were incubated with PBS–2 mM Ca^{2+} (D) or PBS–10 mM EDTA (E) for 10 min at room temperature. Grids were floated on the samples for 5 min at room temperature and stained with 2% PTA, pH 6.5. Bar, 75 nm.

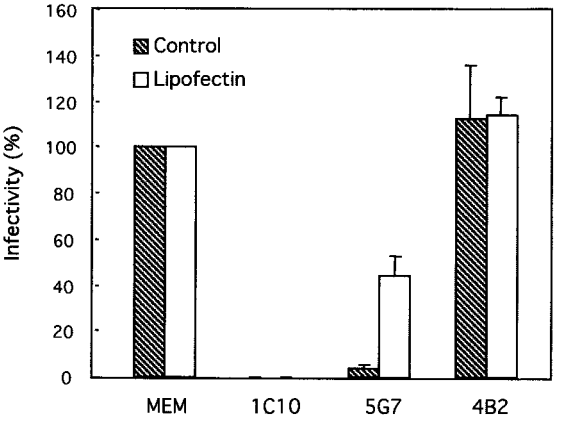

FIG. 8. Liposome-mediated transfections of OSU virions treated with MAbs directed against VP7 (1C10), VP8* (5G7), and VP6 (4B2) in MA-104 cells. Purified OSU virions (20 μg/ml; 10^7 FFU/ml) were mixed with different MAbs (52 μg/ml) and incubated for 1 h at room temperature. Virus-antibody mixtures were divided into two aliquots (50 μl), and each aliquot was treated either with Lipofectin (50 μg/ml) or with MEM, vortexed briefly, and incubated for 20 min at room temperature. The mixtures were serially diluted in MEM and inoculated in duplicate onto MA-104 cells grown in 96-well plates. The next day (12 to 18 h p.i.), the cells were fixed with methanol and immunostained for FFU. Results are expressed as percent infectivity compared with the infectivity of the virus that was not transfected or reacted with antibodies. Results are means ± standard deviations from three experiments conducted on three separate days.

antibodies are not completely understood. In this study, we have obtained evidence indicating that in vitro solubilization of the outer shell of the rotavirus capsid induced by low Ca^{2+} concentrations can be prevented by binding of MAbs directed against VP7 but not by binding of MAbs against VP8* or VP5*. The inhibitory activity of the anti-VP7 neutralizing MAbs was dependent on antibody concentration and on the bivalent binding of the antibody. These findings indicate that antibodies directed against the rotavirus outer capsid protein VP7 neutralize virus infectivity because they prevent decapsidation of the virion, which in turn prevents steps further down in the replication cycle (6).

Neutralization experiments with MAbs directed against VP8* and VP7 of the porcine rotavirus strain OSU indicated that neutralization by these antibodies followed a very different dependence on MAb concentration, suggesting that different mechanisms are involved. Similar results were previously obtained by Ruggeri and Greenberg (32) using the simian rotavirus strain RRV. These authors postulated that the blocking of viral attachment was most likely the mechanism by which MAbs directed against VP4 mediated neutralization. On the other hand, antibodies that neutralized at concentrations below saturation, such as those directed against VP7, probably acted by mechanisms other than inhibition of binding. Since neutralization mediated by a few antibody molecules per virion has been associated with inhibition of structural transitions in other nonenveloped viruses (10, 24), we decided to test whether neutralizing antibodies directed against VP7 were able to inhibit the low-calcium-mediated solubilization of the outer capsid proteins of rotavirus.

In vitro decapsidation of OSU and RRV virions is blocked by neutralizing MAbs that recognize conformationally determined epitopes of VP7 on the virion (5, 39). These results indicate that inhibition of decapsidation may be one of the mechanisms by which neutralizing MAbs directed against VP7 exert their potent action in vivo. The proposed mechanism of action is consistent with previous data, which showed that calcium chelation disrupts complexes of neutralizing MAbs and solubilized VP7, but not when VP7 is attached to the virion (11). In fact, neutralizing anti-VP7 MAbs, such as MAb 159, bind to recombinant expressed VP7 in a Ca^{2+}-dependent fashion (11, 12). However, once VP7 is assembled onto the virion, the neutralization domains are stabilized and the VP7-MAb interaction becomes Ca^{2+} independent (11). In agreement, our results also suggest that rotavirus-MAb interactions are not modified at different Ca^{2+} concentrations, at least down to the Ca^{2+} concentration critical for decapsidation of different strains; rather, this interaction seems to protect virions from decapsidation induced by a reduction in Ca^{2+} concentration.

A clear dose-response effect with the anti-VP7 MAb 1C10 was observed in the scattering as well as the neutralization assays. The relationship between neutralization or decapsidation and the MAb/virus ratio was the same for both effects. This suggests that inhibition of decapsidation is the mechanism of neutralization of infectivity.

Our results are also consistent with numerous observations that MAbs directed against VP7 do not inhibit binding of the rotavirus to the cell and are able to neutralize infectivity even

if they are allowed to act after virus attachment (8, 25, 32). Neutralizing MAbs directed against VP8* have also been demonstrated to block infectivity after virus binding. However, MAbs directed against VP8* exert their postattachment effects by detaching the virus from the cell surface (32). Presumably, they are able to overcome the weak initial interaction between the virion and its receptor via VP8*. On the other hand, the postattachment inhibition activity of the MAbs directed against VP7 observed with RRV did not involve displacement of the virus from the cell surface (32). Postattachment neutralization has been reported for several other nonenveloped viruses (4, 18, 41). Stabilization of the capsid, preventing essential conformational changes, has been suggested as a mechanism of postattachment neutralization of polioviruses and reoviruses (19, 41). In addition, protective MAbs specific to reoviruses inhibit replication and intracellular proteolytic uncoating of the virion independently of effects on binding (18).

Neutralizing antibodies directed against VP7 have also been shown to inhibit TLP-induced cell membrane permeabilization as measured by the coentry of the protein toxin α-sarcin into the cell (8, 25). Solubilization of the outer capsid of trypsinized TLP in the absence of calcium has been proposed as a requirement for the virus to induce destabilization of the membrane (34, 37). The present data suggest that binding of antibodies to VP7 blocks membrane permeabilization indirectly by preventing the solubilization of VP7. In reoviruses, MAbs directed against intermediate subviral particle protein μ1 added postattachment are able to stabilize the virus particle and therefore inhibit permeabilization of L-cell membranes (18, 19). A similar situation has been reported for polioviruses, where compounds that inhibit poliovirus uncoating block the early permeabilization of cell membranes to protein toxins induced by virus particles (1). Together, these data strongly suggest that disassembly of the virion is a necessary step for nonenveloped viruses to achieve membrane permeabilization, a process that has been taken as an indicator of productive virus penetration (8, 13, 19, 25).

The capacity of MAbs directed against VP7 of OSU to inhibit outer capsid solubilization was completely reversed by papain treatment to generate Fab fragments, while $F(ab')_2$ fragments fully retained the capacity to prevent decapsidation. These findings are in complete agreement with previous data showing that papain treatment of RRV neutralized with three different IgG MAbs directed against VP7 led to substantial recovery of infectivity (32). Despite the requirement for bivalent binding of the anti-VP7 MAbs, virion aggregation appears not to be a major mechanism by which these MAbs neutralize rotaviruses. In addition, the role of virion aggregation as a mechanism of protection in vivo has been questioned, because it occurs over a narrow range of antibody/virus ratios (3). The finding that bivalent binding of the antibody is required for neutralization supports the notion that anti-VP7 MAbs exert their effect by stabilizing the virion, presumably by cross-linking adjacent VP7 subunits and impeding conformational changes or rearrangements necessary for the solubilization of the outer capsid proteins (11, 12). The neutralization experiments with OSU and RRV suggest that not all VP7 molecules need to be combined with antibodies for the capsid to be stabilized. The requirement for bivalent binding has been observed for polioviruses and reoviruses, where conformational alteration of the capsid proteins is a necessary step for productive viral entry (18, 41).

The results obtained in the transfection experiments support the idea that OSU virions neutralized via VP7 are not able to decapsidate at the low Ca^{2+} concentration of the cytoplasm. Bass et al. (2) were also unable to recover infectivity after liposome-mediated transfections of RRV virions neutralized via VP7 with MAb 159. Furthermore, the lipofection results suggest that the blockade in decapsidation observed in the scattering experiments in vitro also occurs in live cultured cells.

The mechanism of rotavirus entry into the cell is still unclear. Both direct virion penetration of the cytoplasmic cell membrane (23) and pH-independent, Ca^{2+}-dependent endocytosis (28, 34, 37) have been proposed. Although the data presented here do not allow us to draw conclusions as to the pathway of virus penetration, they suggest that the low Ca^{2+} concentration in the cell cytoplasm is sufficient to induce outer capsid destabilization and infection.

Our data are entirely consistent with the notion that MAbs to VP8* neutralize rotavirus infectivity by inhibiting binding of the virion to the target cell (32). MAbs directed against OSU VP8* showed a neutralization efficiency that was proportional to the concentration of the antibody, suggesting that interaction of the anti-VP8* antibodies with all or most VP8* molecules is a requirement for neutralization to be accomplished. The partial recovery of infectivity observed with transfected OSU virions neutralized via VP8* also supports the hypothesis that neutralizing MAbs directed against VP8* exert their effect by inhibiting the binding of the virion to the cells. The outer capsid protein VP5* has been implicated in the permeabilization of membranes (9, 35). Our data are also consistent with the suggestion that MAbs directed against VP5* may neutralize infectivity by preventing virus-membrane interactions and cellular entry. In these studies, the neutralizing antibodies against VP8* or VP5* that were tested did not inhibit the decapsidation process, even though these antibodies were used at very high (saturating) concentrations.

Calcium plays an important structural role in the stability of the rotavirus capsid by binding within VP7 trimers, which are the basic building blocks of the outer layer of the virion (12). Binding of neutralizing MAbs directed against VP7 may prevent solubilization of the outer capsid by increasing the affinity of the VP7 trimers for calcium. Alternatively, the bound neutralizing MAbs may substitute for calcium in holding together the VP7 layer on the virion. However, this possibility seems unlikely in view of the fact that not all molecules of VP7 need to be combined with antibodies in order to achieve neutralization. Therefore, it is reasonable to assume that the bivalent binding of a few molecules of neutralizing MAbs directed against VP7 results in the prevention of possible changes in VP7 conformation necessary for Ca^{2+} release and decapsidation.

In summary, the present data and the findings of others suggest that neutralizing MAbs against VP7 mediate their neutralizing activity by inhibiting decapsidation of the virion, probably by increasing the affinity for Ca^{2+} and preventing dissociation of the VP7 trimers. Cryelectron microscopy has been used to localize the binding sites for neutralizing MAbs directed against VP8* and VP5* (31, 40). Cryoelectron microscopy images of virus-MAb complexes should lead to identifi-

cation of the topographical location of the epitopes recognized by these MAbs and further explain their mechanism of action.

ACKNOWLEDGMENTS

We thank Ramon Montaño for suggesting the protocols for papain digestion of the antibodies and Fabian Michelangeli for helpful discussions and critical reading of the manuscript. We acknowledge Mirtha Romano, Fredi Sanchez, and Jorge Rivas for assistance with EM and photographic work.

This work was supported in part by FONACIT (Venezuela) grant 2001000329.

REFERENCES

1. **Almela, M. J., M. E. Gonzalez, and L. Carrasco.** 1991. Inhibitors of poliovirus uncoating efficiently block the early membrane permeabilization induced by virus particles. J. Virol. **65:**2572–2577.
2. **Bass, D. M., M. R. Baylor, C. Chen, E. M. Mackow, M. Bremont, and H. B. Greenberg.** 1992. Liposome-mediated transfection of intact viral particles reveals that plasma membrane penetration determines permissivity of tissue culture cells to rotavirus. J. Clin. Investig. **90:**2313–2320.
3. **Che, Z., N. H. Olson, D. Leippe, W. M. Lee, A. G. Mosser, R. R. Rueckert, T. S. Baker, and T. J. Smith.** 1998. Antibody-mediated neutralization of human rhinovirus 14 explored by means of cryoelectron microscopy and X-ray crystallography of virus-Fab complexes. J. Virol. **72:**4610–4622.
4. **Christensen, N. D., N. M. Cladel, and C. A. Reed.** 1995. Postattachment neutralization of papillomaviruses by monoclonal and polyclonal antibodies. Virology **207:**136–142.
5. **Ciarlet, M., M. Hidalgo, M. Gorziglia, and F. Liprandi.** 1994. Characterization of neutralization epitopes on the VP7 surface protein of serotype G11 porcine rotaviruses. J. Gen. Virol. **75:**1867–1873.
6. **Cohen, J., J. Laporte, A. Charpilienne, and R. Scherrer.** 1979. Activation of rotavirus RNA polymerase by calcium chelation. Arch. Virol. **60:**177–186.
7. **Crawford, S. E., M. Labbe, J. Cohen, M. H. Burroughs, Y. J. Zhou, and M. K. Estes.** 1994. Characterization of virus-like particles produced by the expression of rotavirus capsid proteins in insect cells. J. Virol. **68:**5945–5952.
8. **Cuadras, M. A., C. F. Arias, and S. Lopez.** 1997. Rotaviruses induce an early membrane permeabilization of MA104 cells and do not require a low intracellular Ca^{2+} concentration to initiate their replication cycle. J. Virol. **71:**9065–9074.
9. **Denisova, E., W. Dowling, R. LaMonica, R. Shaw, S. Scarlata, F. Ruggeri, and E. R. Mackow.** 1999. Rotavirus capsid protein VP5* permeabilizes membranes. J. Virol. **73:**3147–3153.
10. **Dimmock, N. J.** 1993. Neutralization of animal viruses. Curr. Top. Microbiol. Immunol. **183:**1–149.
11. **Dormitzer, P. R., G. W. Both, and H. B. Greenberg.** 1994. Presentation of neutralizing epitopes by engineered rotavirus VP7's expressed by recombinant vaccinia viruses. Virology **204:**391–402.
12. **Dormitzer, P. R., H. B. Greenberg, and S. C. Harrison.** 2000. Purified recombinant rotavirus VP7 forms soluble, calcium-dependent trimers. Virology **277:**420–428.
13. **Fernandez-Puentes, C., and L. Carrasco.** 1980. Viral infection permeabilizes mammalian cells to protein toxins. Cell **20:**769–775.
14. **Gajardo, R., P. Vende, D. Poncet, and J. Cohen.** 1997. Two proline residues are essential in the calcium-binding activity of rotavirus VP7 outer capsid protein. J. Virol. **71:**2211–2216.
15. **Gilbert, J. M., and H. B. Greenberg.** 1997. Virus-like particle-induced fusion from without in tissue culture cells: role of outer-layer proteins VP4 and VP7. J. Virol. **71:**4555–4563.
16. **Guerrero, C. A., E. Mendez, S. Zarate, P. Isa, S. Lopez, and C. F. Arias.** 2000. Integrin $\alpha v\beta 3$ mediates rotavirus cell entry. Proc. Natl. Acad. Sci. USA **97:**14644–14649.
17. **Hewish, M. J., Y. Takada, and B. S. Coulson.** 2000. Integrins $\alpha 2\beta 1$ and $\alpha 4\beta 1$ can mediate SA11 rotavirus attachment and entry into cells. J. Virol. **74:**228–236.
18. **Hooper, J. W., and B. N. Fields.** 1996. Monoclonal antibodies to reovirus $\sigma 1$ and $\mu 1$ proteins inhibit chromium release from mouse l cells. J. Virol. **70:**672–677.
19. **Hooper, J. W., and B. N. Fields.** 1996. Role of the $\mu 1$ protein in reovirus stability and capacity to cause chromium release from host cells. J. Virol. **70:**459–467.
20. **Hoshino, Y., M. M. Sereno, K. Midthun, J. Flores, A. Z. Kapikian, and R. M. Chanock.** 1985. Independent segregation of two antigenic specificities (VP3 and VP7) involved in neutralization of rotavirus infectivity. Proc. Natl. Acad. Sci. USA **82:**8701–8704.
21. **Isa, P., S. Lopez, L. Segovia, and C. F. Arias.** 1997. Functional and structural analysis of the sialic acid-binding domain of rotaviruses. J. Virol. **71:**6749–6756.
22. **Johnstone, A., and R. Thorpe.** 1987. Immunochemistry in practice, 2nd ed. Blackwell Scientific Publications, Oxford, United Kingdom.
23. **Kaljot, K. T., R. D. Shaw, D. H. Rubin, and H. B. Greenberg.** 1988. Infectious rotavirus enters cells by direct cell membrane penetration, not by endocytosis. J. Virol. **62:**1136–1144.
24. **Krause, R. M., N. J. Dimmock, and D. M. Morens.** 1997. Summary of antibody workshop. The role of humoral immunity in the treatment and prevention of emerging and extant infectious diseases. J. Infect. Dis. **176:**549–559.
25. **Liprandi, F., Z. Moros, M. Gerder, J. E. Ludert, F. H. Pujol, M. C. Ruiz, F. Michelangeli, A. Charpilienne, and J. Cohen.** 1997. Productive penetration of rotavirus in cultured cells induces coentry of the translation inhibitor α-sarcin. Virology **237:**430–438.
26. **Ludert, J. E., N. Feng, J. H. Yu, R. L. Broome, Y. Hoshino, and H. B. Greenberg.** 1996. Genetic mapping indicates that VP4 is the rotavirus cell attachment protein in vitro and in vivo. J. Virol. **70:**487–493.
27. **Ludert, J. E., F. Gil, F. Liprandi, and J. Esparza.** 1986. The structure of the rotavirus inner capsid studied by electron microscopy of chemically disrupted particles. J. Gen. Virol. **67:**1721–1725.
28. **Ludert, J. E., F. Michelangeli, F. Gil, F. Liprandi, and J. Esparza.** 1987. Penetration and uncoating of rotaviruses in cultured cells. Intervirology **27:**95–101.
29. **Matsui, S. M., P. A. Offit, P. T. Vo, E. R. Mackow, D. A. Benfield, R. D. Shaw, L. Padilla-Noriega, and H. B. Greenberg.** 1989. Passive protection against rotavirus-induced diarrhea by monoclonal antibodies to the heterotypic neutralization domain of VP7 and the VP8 fragment of VP4. J. Clin. Microbiol. **27:**780–782.
30. **Mertens, P. P. C., M. Arrella, H. Attoui, et al.** 2000. Family *Reoviridae*, p. 395–480. *In* M. H. V. van Regenmortel, C. M. Fauquet, D. H. L. Bishop, E. B. Carstens, M. K. Estes, S. M. Lemon, J. Maniloff, M. A. Mayo, D. J. McGeoch, C. R. Pringle, and R. B. Wickner (ed.), Virus taxonomy: classification and nomenclature of viruses. Seventh report of the International Committee on Taxonomy of Viruses. Academic Press, San Diego, Calif.
31. **Prasad, B. V. V., J. W. Burns, E. Marietta, M. K. Estes, and W. Chiu.** 1990. Localization of VP4 neutralization sites in rotavirus by three-dimensional cryo-electron microscopy. Nature **343:**476–479.
32. **Ruggeri, F. M., and H. B. Greenberg.** 1991. Antibodies to the trypsin cleavage peptide VP8* neutralize rotavirus by inhibiting binding of virions to target cells in culture. J. Virol. **65:**2211–2219.
33. **Ruggeri, F. M., K. Johansen, G. Basile, J. P. Kraehenbuhl, and L. Svensson.** 1998. Antirotavirus immunoglobulin A neutralizes virus in vitro after transcytosis through epithelial cells and protects infant mice from diarrhea. J. Virol. **72:**2708–2714.
34. **Ruiz, M. C., M. J. Abad, A. Charpilienne, J. Cohen, and F. Michelangeli.** 1997. Cell lines susceptible to infection are permeabilized by cleaved and solubilized outer layer proteins of rotavirus. J. Gen. Virol. **78:**2883–2893.
35. **Ruiz, M. C., S. R. Alonso Torre, A. Charpilienne, M. Vasseur, F. Michelangeli, J. Cohen, and F. Alvarado.** 1994. Rotavirus interaction with isolated membrane vesicles. J. Virol. **68:**4009–4016.
36. **Ruiz, M. C., A. Charpilienne, F. Liprandi, R. Gajardo, F. Michelangeli, and J. Cohen.** 1996. The concentration of Ca^{2+} that solubilizes outer capsid proteins from rotavirus particles is dependent on the strain. J. Virol. **70:**4877–4883.
37. **Ruiz, M. C., J. Cohen, and F. Michelangeli.** 2000. Role of Ca^{2+}in the replication and pathogenesis of rotavirus and other viral infections. Cell Calcium **28:**137–149.
38. **Shaw, A. L., R. Rothnagel, D. Chen, R. F. Ramig, W. Chiu, and B. V. Prasad.** 1993. Three-dimensional visualization of the rotavirus hemagglutinin structure. Cell **74:**693–701.
39. **Shaw, R. D., P. T. Vo, P. A. Offit, B. S. Coulson, and H. B. Greenberg.** 1986. Antigenic mapping of the surface proteins of rhesus rotavirus. Virology **155:**434–451.
40. **Tihova, M., K. A. Dryden, A. R. Bellamy, H. B. Greenberg, and M. Yeager.** 2001. Localization of membrane permeabilization and receptor binding sites on the VP4 hemagglutinin of rotavirus: implications for cell entry. J. Mol. Biol. **314:**985–992.
41. **Wetz, K.** 1993. Attachment of neutralizing antibodies stabilizes the capsid of poliovirus against uncoating. Virology **192:**465–472.
42. **Yeager, M., J. A. Berriman, T. S. Baker, and A. R. Bellamy.** 1994. Three-dimensional structure of the rotavirus haemagglutinin VP4 by cryo-electron microscopy and difference map analysis. EMBO J. **13:**1011–1018.
43. **Zhou, Y. J., J. W. Burns, Y. Morita, T. Tanaka, and M. K. Estes.** 1994. Localization of rotavirus VP4 neutralization epitopes involved in antibody-induced conformational changes of virus structure. J. Virol. **68:**3955–3964.